Submitted, accepted and published by:
Fuel Processing Technology 90 (2009) 1471–1479

Syngas combustion in a 500 W_{th} Chemical-Looping Combustion system using an impregnated Cu-based oxygen carrier

C. R. Forero[a], P. Gayán*, L. F. de Diego, A. Abad, F. García-Labiano, J. Adánez

Instituto de Carboquímica (C.S.I.C.), Dept. of Energy & Environment, Miguel Luesma Castán, 4, Zaragoza, 50018, Spain

[a] University of Valle, Engineering School of Natural and Environmental Resources (EIDENAR). Calle 13 No. 100-00, 25360 Cali, Colombia.

* Corresponding authors: Tel: (+34) 976 733 977. Fax: (+34) 976 733 318. E-mail addresses: pgayan@icb.csic.es (Pilar Gayán)

Syngas combustion in a 500 W_{th} Chemical-Looping Combustion system using an impregnated Cu-based oxygen carrier

C. R. Forero[a], P. Gayán*, L. F. de Diego, A. Abad, F. García-Labiano, J. Adánez

Instituto de Carboquímica (C.S.I.C.), Dept. of Energy & Environment, Miguel Luesma Castán, 4, Zaragoza, 50018, Spain

[a] University of Valle, Engineering School of Natural and Environmental Resources (EIDENAR). Calle 13 No. 100-00, 25360 Cali, Colombia.

* Corresponding authors: Tel: (+34) 976 733 977. Fax: (+34) 976 733 318. E-mail addresses: pgayan@icb.csic.es (Pilar Gayán)

ABSTRACT

Chemical-Looping Combustion (CLC) is an emerging technology for CO_2 capture because separation of this gas from the other flue gas components is inherently to the process and thus no energy is expended for the separation. For its use with coal as fuel in power plants, a process integrated by coal gasification and CLC would have important advantages for CO_2 capture. This paper presents the combustion results obtained with a Cu-based oxygen carrier in a continuous operation CLC plant (500 W_{th}) using syngas as fuel. For comparison purposes pure H_2 and CO were also used. Tests were performed at two temperatures (1073 and 1153 K), different solid circulation rates and power inputs. Full syngas combustion was reached at 1073K

working at ϕ higher than 1.5. The syngas composition had small effect on the combustion efficiency. This result seems to indicate that the water gas shift reaction acts as an intermediate step in the global combustion reaction of the syngas. The results obtained after 40 hours of operation showed that the copper-based oxygen carrier prepared by impregnation could be used in a CLC plant for syngas combustion without operational problems such as carbon deposition, attrition, or agglomeration.

Keywords

CO_2 capture, chemical-looping combustion, syngas, copper, oxygen carrier.

1. INTRODUCTION

Fossil fuel combustion is the main contributor to increase atmospheric CO_2 concentrations, an important greenhouse gas that contributes to global climate change [1]. About a third of the global CO_2 emissions come from the burning of fossil fuels in power generation. Among the different technologies that are under development, Chemical-Looping Combustion (CLC) has been suggested as one of the most promising technologies for reducing the cost of CO_2 capture using fuel gas [2,3] because CO_2 is inherently separated in the process from the other flue gas components (N_2 and unused O_2) and thus no energy is expended for the separation.

CLC is a two-step gas combustion process that produces a pure CO_2 stream, ready for compression and sequestration. A solid oxygen carrier (OC) circulates between two reactors and transports oxygen from the combustion air to the fuel. Since the fuel is not mixed with air, the subsequent CO_2 separation process is not necessary. The most common design of a CLC plant includes a high-velocity riser for the air reactor (AR)

and a low-velocity fluidized bed for the fuel reactor (FR), with the oxygen carrier in the form of metal oxide particles circulating between them.

In this system, the total amount of heat evolved from reactions in the two reactors is the same as for normal combustion, where the oxygen is in direct contact with fuel. Using syngas as fuel, reduction and oxidation reactions are exothermic; therefore, the circulation rates in the system are mainly based on the oxygen necessary to achieve high fuel conversion [4]. For a copper-based oxygen carrier and syngas as fuel the reduction and oxidation reactions are shown below. In the FR, the metal oxide is reduced by the following reactions:

$$H_2 + CuO \longleftrightarrow Cu + H_2O \qquad \Delta H^0c = -85.8 \text{ kJ/mol} \qquad (1)$$

$$CO + CuO \longleftrightarrow Cu + CO_2 \qquad \Delta H^0c = -126.9 \text{ kJ/mol} \qquad (2)$$

Particles of the oxygen carrier are transferred to the AR where they are regenerated by taking up oxygen from the air:

$$O_2 + 2Cu \longleftrightarrow 2CuO \qquad \Delta H^0c = -312.1 \text{ kJ/mol} \qquad (3)$$

The oxidized carrier is recirculated to the fuel reactor for a new cycle.

Natural gas, refinery gas, synthesis gas from coal gasification, or residual streams from pressure swing adsorption (PSA) units in H_2 separation can be used as gaseous fuels in the CLC process. The CLC process has been demonstrated for natural gas in plants at scales of 10 kW [5-8], 50 kW [9] and 120 kW [10]. Recently, as coal is a much more abundant fossil fuel in comparison to natural gas, interest has arisen about combustion of solid fuels. There are two possibilities for the use of the CLC technology with coal. The first one is direct combustion in the CLC process, where the gasification of coal and the subsequent reactions of gasification gases with the oxygen carrier particles will occur simultaneously in the same reactor [11-14]. The efficiency of char

gasification in the fuel reactor and the separation of ash from oxygen carrier are the key factors for the development of this process. The second possibility for the use of coal can be easily accomplished by a process integrating coal gasification and chemical-looping combustion (IGCC-CLC) [15, 16]. In this process, the syngas produced from coal gasification is used as fuel in a CLC system for power generation with CO_2 capture. Simulations made by Jin and Ishida [16] and Wolf et al. [17] showed that this process have the potential to achieve an efficiency of about 5-10% points higher than a similar integrated gasification combined cycle process (IGCC) that uses conventional CO_2 capture technology.

Continuous units have been designed and operated for the use of syngas in a 300-500 W [18-21], where different oxygen carriers based on Mn-, Fe- , and Ni-, were successfully tested. However, the selection of the oxygen carrier is a key factor for the CLC technology development. Among the different metal oxides proposed in the literature for the CLC process, Cu-based oxygen carriers have shown high reaction rates and oxygen transfer capacity [22], and have no thermodynamic restrictions for complete fuel conversion to CO_2 and H_2O. In addition, the use of Cu-based oxygen carriers does not have the environmental problems associated with the use of Ni-based OC. Another advantage of using copper is the low metal price in comparison to nickel.

Our research group at the Instituto of Carboquímica (CSIC) has undertaken several studies using oxygen carriers based on copper. In previous works potential Cu-based oxygen carriers were prepared using different supports [23]. The effects of oxygen carrier composition and preparation method were also investigated in a TGA [24] to develop oxygen carriers with high reaction rates and durability. It was found that the optimum preparation method for Cu-based oxygen carriers was the impregnation on a

support. Later, the preparation conditions and oxygen carrier characteristics were optimized to avoid the agglomeration of the Cu-based materials during their operation in a fluidized bed [25], which was the main reason adduced in the literature to reject this kind of materials for their use in a CLC process. Based on these findings, an oxygen carrier was finally selected to test its behaviour in a 10 kW_{th} CLC prototype using methane as fuel. The results obtained during 200 h of continuous operation were very successful both regarding methane combustion efficiencies and particle behaviour [6,7]. Finally, a waste management study from the CLC plant using Cu-based residues was also carried out [26]. It was concluded that this solid residue can be classified as a stable non-reactive hazardous waste acceptable at landfills for non-hazardous wastes.

The aim of this work was to evaluate the behaviour of this Cu-based oxygen carrier prepared by impregnation for the syngas combustion. To this end, a 500 W_{th} continuously operated CLC unit was used. The effect on the combustion efficiency of different operating variables, such as syngas composition, solids circulation rate, power input and fuel reactor temperature has been determined. The gas leakage, carbon deposition, particle attrition or agglomeration behaviour during the tests were also evaluated.

2. EXPERIMENTAL SECTION

2.1. Oxygen Carrier

An oxygen carrier based on copper and Al_2O_3 as support was prepared by the incipient wetness impregnation method. The material was prepared by the addition of a volume of saturated copper nitrate solution (5.4 M) corresponding to the total pore volume of the support particles. Commercial γ-alumina particles (Puralox NWa-155, Sasol Germany GmbH) with a density of 1.3 g/cm^3, a porosity of 55.4 % and sieved to a

size range of 300-500 μm were used as support. The aqueous solution was slowly added to the support particles, with thorough stirring at room temperature. The oxygen carrier was subsequently calcined for 30 min at 823 K in a muffle oven to decompose the impregnated copper nitrate into copper oxide. Finally, the oxygen carrier was stabilized in air atmosphere for 1 hour at 1123 K, obtaining a material whose main characteristics are shown in Table 1. The oxygen transport capacity, that is, the mass fraction of oxygen that can be used in the process, was defined as:

$$R_{OC} = \frac{\left(m_{ox} - m_{red}\right)}{m_{ox}} \tag{4}$$

where m_{ox} and m_{red} are the masses of the oxidized and reduced form of the metal oxide, respectively.

2.2 Characterization of Oxygen Carrier

Several techniques have been used to characterize the fresh and after-use oxygen carrier particles. Particle porosity was measured by Hg intrusion in a Quantachrome PoreMaster 33, and specific surface area was determined by N_2 physisorption using a Micromeritics ASAP-2020 apparatus. The force needed to fracture a particle was determined using a Shimpo FGN-5X crushing strength apparatus. The crushing strength value was taken as the average value of at least 20 measurements. The identification and quantitative analysis of crystalline phase of the samples were carried out by powder X-ray diffraction (XRD) Bruker AXS D8 Advance, equipped with monochromatic beam diffracted graphite, using Ni-filtered "Cu Kα" radiation.

Reactivity tests and experiments to determine the oxygen transport capacity, R_{OC}, of the oxygen carrier have been carried out in a thermogravimetric analyzer (TGA) CI Electronics Ltd. Detailed information about the instrument and operating procedure used can be found elsewhere [27].

To determine the reactivity of the oxygen carrier with syngas, two different CO/H_2 ratios ranging from 1 to 3 were used. Table 2 shows the gas concentration used in the experiments. H_2O and CO_2 were introduced in the concentrations determined by the water-gas shift (WGS) equilibrium at the reacting temperature. For comparison purposes, the reactivity of the oxygen carrier with pure H_2 or CO was also determined. CO_2 was introduced together with CO to avoid carbon formation by the Boudouard reaction. In all cases, nitrogen was used to balance. For oxidation reaction, 100% air was used as reacting gas. The TGA experiments were always carried out at 1073 K. To prevent the fuel mixing with air, a nitrogen flow was passed for two minutes after each oxidizing and reducing periods.

2.3 Experimental 500 W_{th} CLC pilot plant

Figure 1(a) shows a schematic diagram of the reactor system, which was designed and built at Instituto of Carboquímica (CSIC). The atmospheric Chemical-Looping Combustor continuous unit was composed of two interconnected fluidized-bed reactors separated by a loop seal, a riser for solids transport to the fuel reactor, a cyclone and a solid valve to control the flowrate of solids fed to the fuel reactor. This design allowed the variation and control of the solids circulation rate between both reactors. The FR, (A) consisted of a bubbling fluidized bed (0.05 m i.d.) with a bed height of 0.1 m. In this reactor the fuel combustion was performed by the oxygen carrier, giving CO_2 and H_2O according to Eqs. (1) and (2). Reduced oxygen carrier particles overflowed into the AR (C), through an U-shaped fluidized loop seal (B, LS_{bottom}), to avoid gas mixing between fuel and air. The oxidation of the carrier took place at the AR, which consisted of a bubbling fluidized bed (0.05 m i.d.) with a bed height of 0.1 m. It was followed by a riser (D) of 0.02 m i.d. and 1 m height. The regeneration of the oxygen carrier

happened in the dense bed of the AR allowing residence times high enough for the complete oxidation of the reduced carrier, according to Eq. (3). Secondary air could be introduced at the top of the bubbling bed to help particle entrainment. N_2 and unreacted O_2 left the AR passing through a high-efficiency cyclone (E) and a filter (F) before the stack. The solid particles recovered by the cyclone were sent to a solid reservoir (S_{up}) setting the oxygen carrier ready to start a new cycle and avoiding the mixing of fuel and air out of the riser. The regenerated oxygen carrier particles returned to the FR by gravity from the solid reservoir located above a solids valve (G) which controlled the solids circulation rate entering the FR. A diverting solids valve (H) located below the cyclone allowed the measurement of the solid flow rates at any time. Fine particles produced by fragmentation/attrition in the plant were recovered in the filters that were located downstream of the FR and AR.

The prototype had several tools of measurement and system control. Thermocouples and pressure drop transducers located at different points of the plant showed the current operating conditions in the plant at any time. Specific mass flow controllers gave accurate flow rates of feeding gases. The gas outlet streams of the FR and AR were drawn to respective on-line gas analyzers to get continuous data of the gas composition. CO, CO_2 and H_2, concentrations in the gas outlet stream from the FR were measured after steam condensation. O_2, CO, and CO_2 concentrations were obtained at the gas outlet stream from the AR. CO and CO_2 concentrations were measured by non-dispersive infrared (NDIR) analyzers (Maihak S710 / UNOR), O_2 concentration was determined using a paramagnetic detector (Siemens Oxymat 5E), and H_2 concentration by a thermal conductivity detector (Maihak S710 / THERMOR). All data were collected by means of a data logger connected to a computer.

2.3.1 Pressure profile of the pilot plant

Monitoring pressure drops along the plant gives useful information about the fluidization conditions in the CLC plant, more indeed in this case where two interconnected FB reactors are operating. The pressure balance affects the operation of a CLC system in a double way. On the one hand, it avoids the gas leakage between the reactors. The leakage from the FR to the AR means that the efficiency of carbon capture will be reduced. The leakage from the AR to the FR means that carbon dioxide will be diluted with air, which will reduce the purity of the CO_2 and therefore will increase the cost of CO_2 capture. By the other hand, the pressure balance is important to get the desired solids circulation rate in the system. It must be considered that the solids circulation rate controls the amount of oxygen fed into the FR for the fuel combustion.

The pressure drop profile in the system was measured for different solid fluxes. As an example, Figure 1(b) shows the profile obtained for a solid circulation rate of 6 kg/h. Points 1-2-11 and 6-7-8 represent the upper and bottom seals respectively. The axial pressure profile in the FR is shown by points 9-10-11 and points 5-4-3-1 represents the profile in the AR and riser. It can be seen that the loop seals balance the pressures difference between the reactors. During all tests easy and stable operation of the plant was found. In addition, no gas leakages between the air and fuel reactors were detected.

2.4 Combustion tests

CLC tests under different operating conditions were carried out using the Cu-based oxygen carrier and syngas as fuel. The solid inventory in the system was about 1.1 kg of OC. The inlet gas flow in the FR was 260 lN/h with a gas velocity of 0.14 m/s, which were about 2.5 times the minimum fluidization velocity of the particles. The fuel gas in

the FR was syngas diluted in nitrogen, and no steam was added. Nitrogen was used as a fluidizing agent in the bottom loop seal (45 lN/h).

Air was used as fluidizing gas in the AR. To achieve complete oxidation of the reduced oxygen carrier in the AR, the air was divided into the fluidizing gas in the bottom bed (584 lN/h), allowing high residence times of the particles, and into the secondary air in the riser (165 lN/h) to help particle entrainment.

Air flow into the AR was maintained constant for all tests, remaining always in excess over the stoichiometric oxygen demanded by the fuel gas. The air excess ratio, λ defined in Eq. (5), ranged from 1.5 to 2.6 depending on the fuel flow.

$$\lambda = \frac{\text{Oxygen flow}}{\text{Oxygen demand}} = \frac{0.21 F_{air}}{0.5 (F_{CO} + F_{H_2})} \quad (5)$$

The usual operating temperature was 1073 K in the FR and 1223 K in the AR. Some additional tests were carried out at 1153 K to analyze the effect of the FR temperature. Temperatures in FR and AR were kept constant during operation. A total of about 40 hours at hot conditions, of which 35 hours corresponded to combustion, were carried out using the same batch of oxygen carrier particles. The steady state conditions were maintained at least during 60 min for each operating condition.

The combustion efficiency, defined in Eq. (6), was used to evaluate the behaviour of the oxygen carrier in the combustion of syngas. The combustion efficiency (η_c) was defined as the ratio of the oxygen consumed by the gas leaving the FR to that consumed by the gas when the fuel is completely burnt to CO_2 and H_2O. So, the ratio gives an idea about how the CLC operation is close or far from the full combustion of the fuel, i.e. η_c = 100%.

$$\eta_C = \frac{\left(2x_{CO_2} + x_{CO} + x_{H_2O}\right)_{out} F_{out} - \left(2x_{CO_2} + x_{CO}\right)_{in} F_{in}}{\left(x_{CO} + x_{H_2}\right)_{in} F_{in}} \quad (6)$$

where F_{in} is the molar flow of the inlet gas stream, F_{out} is the molar flow of the outlet gas stream, and x_i is the molar fraction of the gas i corresponding to the inlet or outlet.

The oxygen carrier to fuel ratio (ϕ) was defined by Eq. (7), where F_{CuO} is the molar flow rate of the metal oxide and F_{Fuel} is the inlet molar flow rate of the fuel in the FR. A value of $\phi = 1$ corresponds to the stoichiometric CuO amount needed for a full conversion of the fuel to CO_2 and H_2O:

$$\phi = \frac{F_{CuO}}{\left(x_{CO} + x_{H_2}\right) F_{in}} \quad (7)$$

In the prototype, the effect on the syngas combustion efficiency of different operating variables was analyzed. Table 3 shows a summary of the different operating conditions used in the tests. Moreover, the experiments allow studying the behaviour of the OC with respect to carbon formation, particle attrition, and agglomeration processes.

The syngas composition coming from gasification processes depends on the pressure and temperature conditions, according to the fuel and the gasifying agents (air, oxygen, or steam). The CO/H_2 molar ratios expected from commercial gasifiers range from 1 to 3 [28]. In this work, different syngas compositions inside this range were used to analyze its effect on the combustion with a Cu-based oxygen carrier. Pure H_2 and CO were also used for comparison purposes; CO_2 was always introduced together with CO to avoid carbon formation by the Boudouard reaction (Eq. 8). The syngas composition for the different CO/H_2 molar ratios was selected to fulfil the Water Gas Shift equilibrium (WGS), Eq.9, at the operating temperature, which was assumed immediately achieved at the inlet of the FR.

$$2CO \leftrightarrow CO_2 + C \quad (8)$$

$$CO + H_2O \leftrightarrow CO_2 + H_2 \quad (9)$$

The effect of gas composition on the combustion efficiency has been studied for two different CO/H_2 ratios, 3 and 1 (tests 1 and 2). For comparison purposes, experiments using pure H_2 or CO as gas fuel were also done (tests 3 and 4). The oxygen demand in the FR to get complete combustion of the syngas was the same in these tests (see Table 3).

The effect of the oxygen carrier to fuel ratio (ϕ) on the combustion efficiency (η_c) was analyzed in two ways. By one hand, several experiments were performed using different solids circulation rates (f_s) and maintaining all the other experimental conditions constant (tests 1, 5, and 6). A syngas composed by 40 vol.% CO and 18 vol.% H_2 ($CO/H_2 = 3$) was used. The circulation rates, controlled by the solids valve, were varied over a range of ϕ ratios of 1.1-1.6. Tests 7-12 corresponding to pure gases, H_2 or CO, with the same amount of combustible gas, were used for comparison purposes.

On the other hand, other experimental tests were carried out varying the fuel flow but keeping constant the solids circulation rate, ≈6 kg/h (tests 13-15 for $CO/H_2 = 1$, and tests 16-18 for $CO/H_2 = 3$). Different syngas concentrations ranging from 45 to 70 vol.%, corresponding to power input between 400 and 630 W_{th}, were used at two CO/H_2 ratios. It must be pointed out that experiments were carried out at different power inputs, but maintaining approximately constant the solids inventory in the FR (≈ 0.2 kg) and the air flow in the AR. Therefore, as the fuel flow increased, the oxygen carrier to fuel ratio and the solids inventory in the FR per MW of fuel gas, m^*_{FR}, decreased.

The effect of the FR temperature on combustion efficiency was analyzed at 1073 K and 1153 K (tests 1, 16-18, and 19-22) maintaining constant the CO/H_2 ratio of 3 and varying the power input between 400 – 700 W_{th}.

3. RESULTS AND DISCUSSION

The 500W_{th} chemical-looping combustor has been operated using syngas as fuel and a Cu-based oxygen carrier. The results are presented analyzing the reactivity of the oxygen carrier in the TGA and its behaviour in the CLC pilot plant during 40 hours of continuous operation with respect to agglomeration, attrition, and other types of operational problems. The effect on the combustion efficiency of the syngas composition, the oxygen carrier to fuel ratio, and the temperature of the FR were analyzed.

3.1 Reactivity on TGA

Reactivity tests of both fresh oxygen carrier particles, i.e. particles not subjected to CLC operation, and particles used in the 500 W_{th} CLC prototype, were carried out in the TGA. Figure 2 shows the reduction and oxidation conversions versus time curves obtained using pure H_2, pure CO and different CO/H_2 ratios for the fresh particles. As it can be seen, the reduction reactivity of the fresh oxygen carrier was high with all the fuels although some minor differences were observed depending on the gas used. The highest reactivity was observed for H_2 and the lowest was for CO. These results agree with the ones obtained by Abad et al. [22], who determined that the reactivity of a Cu-OC was higher using H_2 than CO as a gas reducer. The reactivity for the different syngas compositions was high and similar to the reactivity of pure H_2. Moreover the oxygen carrier showed very high reactivity during oxidation.

Similar reactivity results in the TGA were found for the used particles, indicating the Cu-based oxygen carrier maintains its high reactivity after 40 h of operation in the CLC plant.

3.2 Tests in CLC 500 W_{th} pilot plant

To analyze the behaviour of the Cu-based oxygen carrier during syngas combustion, several tests under continuous operation were carried out at different operation conditions. Table 3 shows the main data for the experiments carried out.

As an example, Figure 3 shows the evolution with time of the gas product distribution from the FR and AR for experimental test 16 using syngas as fuel (CO/H_2= 3). The temperatures in the FR and AR were 1073 K and 1223 K, respectively and the solids circulation rate was 6 kg/h, corresponding to a ϕ value of 2.0.

The outlet gas concentrations and the temperatures were maintained uniform during the whole combustion time. As it can be seen, the gas outlet concentrations in FR shows full conversion of syngas (H_2=0 vol.%, CO=0 vol.%) . The CO_2 concentration (≈ 48.5 vol.% in dry basis) was a bit lower than the theoretical value (≈ 53.6 vol.% in dry basis) as a consequence of the dilution produced by N_2 coming from the bottom loop seal. Mass balances were found to be accurate by using the measurements of the gas analyzers from the AR and FR.

Carbon formation during continuous operation in the CLC plant was also analyzed. Carbon deposited on particles could be transported to the AR, where it will be released as CO_2 by air combustion. In this case, the carbon capture efficiency of the CLC unit will be reduced. Carbon deposition on particles could happen in the FR via CO decomposition. In the CLC plant carbon formation was evaluated by measuring the CO and CO_2 concentrations at the outlet from the AR. As there was not gas leakage from the

FR to the AR, any carbon containing gas present in the AR outlet should come from combustion of the solid carbon deposited on the oxygen carrier particles. CO and CO_2 were never detected in the AR outlet stream in any test, indicating the absence of carbon formation at relevant extension in the system.

3.2.1. Oxygen carrier behaviour

A total of about 40 h at hot conditions, of which 35 h corresponded to combustion conditions, was carried out using the same batch of oxygen carrier particles.

During operation, agglomeration or any other type of operational problems were never detected. Moreover, it must be considered that all the tests were carried out using a temperature in the AR of 1223 K and some additional tests at 1153 K in the FR. These temperatures are higher that the ones usually reported for the Cu-based oxygen carriers. However, the behaviour of the oxygen carrier used in this work with respect to chemical stability and reactivity was very satisfactory. More indeed, the high temperature used in the AR did not negatively affect to the agglomeration process of the carrier. In a previous work [25], the authors had also found adequate particle behaviour during a multicycle test at 1223 K in a batch fluidized bed using a similar Cu-based oxygen carrier.

Attrition or fragmentation of particles was analyzed during the syngas CLC process. Particles elutriated from the fluidized bed reactors during operation were recovered in the cyclones and filters and weighted to determine the attrition rate. It was assumed as attrition those particles of size under 40 μm. Figure 4 shows the evolution with time of the attrition rate of the oxygen carrier during the whole operation in the plant. The generation of fine particles was high at the beginning of the operation but, after 12 h of operation a low and constant value of the attrition rate was reached (~0.02 wt.%/h). This

value is in accordance with the ones measured during 100 h of operation in a 10 kW CLC plant using methane as fuel and a similar Cu-based oxygen carrier [7].

Physical and chemical properties of the oxygen carrier particles after the CLC operation were compared to those of fresh particles (see Table 1). The oxygen carrier density increased from 1.6 g/cm^3 to 1.9 g/cm^3 after 40 h of operation. The BET specific surface area decreased from 77 m^2/g to 5 m^2/g after CLC operation, suggesting that some thermal sintering is occurring in the particles due to the high operational temperatures used in FR and AR. The crushing strength decreased from 2.4 N to 1.8 N after operation. However, the attrition rate measured in the plant stabilized at a low value, indicating the mechanical strength of the used particles could be enough for its use in the CLC process. Powder XRD patterns of the fresh carrier, shown in Table 1, revealed the presence of $CuAl_2O_4$, and γ-Al_2O_3 as major crystalline phases and minor amounts of CuO. The powder XRD patterns of used carriers revealed the transformation of the γ-Al_2O_3 to α-Al_2O_3 as a most stable phase at high temperature, explaining the observed evolution of the textural properties of the used oxygen carrier. The interaction of copper with the support is revealed through the formation of copper aluminates that are present in the fresh and after-use particles although the reactivity of the particles was maintained.

3.2.2. Effect of syngas composition

The effect of the syngas compositions on the combustion efficiency has been studied for two different CO/H_2 molar ratios, 1 and 3, corresponding to typical gas compositions obtained in coal gasification processes [28]. For comparison purposes, experiments using pure H_2 and CO as fuel gas were also analyzed. The gas compositions used in the experiments were shown in Table 3, tests 1-4.

Figure 5 shows the combustion efficiency obtained in the continuous plant for the different fuel composition above mentioned. The highest efficiency was obtained using pure H_2 and the lowest with CO. These results are consistent with the results obtained in the reactivity analysis, where it was found that the oxygen carrier reactivity is higher with H_2 than with CO. However, it is remarkable the high and similar efficiencies obtained for the two syngas compositions, even considering the high CO concentration existent in the fuel gas ratio $CO/H_2 = 3$. In a previous work [21] using syngas as fuel and a Ni-based oxygen carrier, the authors have found that only the oxygen carrier reactivity with CO could not explain the high combustion efficiencies obtained in a CLC plant. It was concluded that the water gas shift reaction plays an important role in the global reaction of syngas combustion in a CLC plant when a Ni-based oxygen carrier was used. In this sense, the high combustion efficiency found in this work with CO/H_2 fuel ratio of 3 seems to indicate that this mechanism could be also responsible for the CO combustion when Cu-based oxygen carriers are used.

Figure 6 shows the CO and H_2 concentrations obtained at the outlet of the FR for the experiments carried out with syngas. In all cases, the flue gases almost fulfilled the WGS equilibrium at the operating temperature. For the experiments carried out with CO/H_2 ratio of 3, the CO concentration was higher than H_2, as it was expected due to its lower reactivity. However, for the experiments carried out with CO/H_2 ratio of 1, H_2 concentration was higher than CO. TGA reactivity analysis had shown that H_2 reacts faster than CO. The faster disappearance of the H_2 by the reaction with the oxygen carrier shifts the WGS equilibrium towards the formation of more H_2 and CO_2, also increasing the CO consumption. This suggests that this gas phase reaction acts as an intermediate step in the whole reaction of the oxygen carrier with the syngas fuel. On

the other hand, the linked action of gas–solid and WGS reactions could explain the similar efficiencies obtained during syngas combustion even for very different gas compositions and in presence of high concentrations of the low reactive CO.

3.2.3 Effect of oxygen carrier to fuel ratio (ϕ)

To study the effect of the oxygen carrier/fuel ratio, ϕ, on the gas combustion efficiency several experiments were performed using different solid circulation rates and maintaining all the other experimental conditions constant. A syngas CO/H_2 ratio of 3 and a temperature of 1073 K in the FR were selected. The circulation rate of the oxygen carrier particles was varied over a range of 4.3-6.0 kg/h, which corresponded to ϕ ratios of 1.1 to 1.6. Figure 7 shows the effect of the ϕ value on the combustion efficiency for a CO/H_2 ratio of 3. The effect when using pure H_2 and CO fuel gases were also showed for comparison purposes. Syngas was fully converted working at ϕ values above 1.5. When the ϕ value decreased, the combustion efficiency also decreased because of the lower oxygen availability in the FR. Similar results of the effect of ϕ on the combustion efficiency were found for pure H_2 or CO as gas fuel. Full combustion efficiencies were obtained working at ϕ higher than 1.2 and 2.0 for H_2 and CO, respectively. Combustion efficiencies were very low when CO was used as fuel; this result could be anticipated from the results shown above of the effect of syngas composition.

When the ϕ value decreased below 1.5 for syngas fuel, the combustion efficiency sharply decreased even though the oxygen available in the FR was higher than the oxygen needed to fully convert fuel gas to CO_2 and H_2O ($\phi > 1$). This fact was because the average reactivity of particles in the FR sharply decreased for values $\phi < 1.5$-2.0, and therefore the solids inventory in the FR needed to fully convert the fuel gas strongly

increases [4]. Note that, assuming full oxidation of particles in the AR, the ϕ value is related to the variation of the solid conversion in the reactor, ΔX_S, and the conversion of the oxygen carrier in the FR, X_r, as follows

$$\Delta X_S = X_r = \frac{\eta_c}{\phi} \tag{10}$$

Another experimental test series was carried out varying the fuel flow but keeping the solid circulation rate approximately constant (6 kg/h). Figure 8 shows the effect of the oxygen carrier to fuel ratio on the combustion efficiency when the power input changed in the range of 400-630 W_{th} using two different syngas compositions.

Qualitatively, the results were similar to those obtained when the solids circulation rate was varied. Combustion efficiencies of 100% were obtained for ϕ about 1.6 for both CO/H_2 ratios. Decreasing the ϕ value decreases the combustion efficiency, being this effect more noticeable at lower ϕ ratios. Higher combustion efficiency was found for $CO/H_2 = 1$ at the same ϕ ratio. However, small differences were obtained for the two syngas compositions, even considering the high CO concentration existent in the fuel gas with CO/H_2 ratio of 3, which is according with the results shown above of the effect of syngas composition.

It must be pointed out that experiments shown in Figure 8 were carried out at different power input, increasing the fuel concentration, but maintaining approximately constant the solids inventory in the FR (≈ 0.2 kg) and the air flow in the AR. Therefore, as the fuel flow increased, the ϕ ratio and the solids inventory in the FR per MW of fuel gas, m^*_{FR}, decreased. During operation, it was possible to extract some of oxygen carrier particles coming from the AR, after cyclone separation. For every sample, the oxidation conversion was determined by TGA. It was found that the oxygen carrier was fully

oxidized in the AR in all cases. So, the air to fuel ratio, λ, did not have any influence on the experimental results. Nevertheless, the decrease in ϕ and m^*_{FR} should produce a decrease in the combustion efficiency. So, from results shown in Figure 8 it is difficult to relate the effect of the power input on the combustion efficiency to a change in the ϕ ratio, in m^*_{FR}, or in fuel concentration.

To elucidate the importance of the solids inventory, a comparison between these results and the results obtained from experimental test series varying f_S is also shown in Figure 8. The m^*_{FR} value for each experimental test is also indicated in the figure. It can be seen that, at constant ϕ, the combustion efficiency for test when the fuel flow changed, was lower than for experiments where the fuel flow was constant. Differences between series can be resumed in changes on the solids inventory per MW of fuel gas, m^*_{FR}, and on the fuel concentration.

On the one hand, the increase of the combustion efficiency when the ϕ value increases, was higher when the fuel flow was changing. Indeed, for ϕ > 1.4 the effect of ϕ on the combustion efficiency was more noticeable when the syngas flow was changed. This result agrees with results showed in a previous work [4] where it was shown that the average reactivity of particles in the reactor scarcely changed when the variation of the solid conversion in the reactor, ΔX_S, was lower than 0.5-0.6, corresponding to ϕ >1.5-2.0. This fact suggests that for ϕ values in range 1.4-1.6 an increase in the solids inventory in the FR should have a higher influence on the combustion efficiency than an increase in the solids circulation rate. By the other hand, a higher concentration should increase the combustion efficiency when m^*_{FR} was constant, whereas a m^*_{FR} decrease affects negatively to the combustion efficiency. From

results showed in Figure 8, it can be concluded that the negative effect of the decrease of m^*_{FR} on the combustion efficiency was higher than the positive effect of the increase of fuel concentration. Therefore, it can be concluded that the solids inventory, m^*_{FR}, has a high relevance on the combustion efficiency, whereas the solids circulation rate became also important at $\phi < 1.4$.

3.2.4. Effect of temperature

The effect of fuel reactor temperature was studied in the CLC plant. Figure 9 shows the effect of the oxygen carrier to fuel ratio on the combustion efficiency at two FR temperatures (1073 and 1153 K) with a syngas CO/H_2 ratio of 3 and varying the power input.

An increase in the fuel reactor temperature produced an increase in the combustion efficiency. This effect was due to higher oxygen carrier reactivity as a consequence of the dependence of the kinetic constant with the temperature. Obviously, to obtain complete combustion of the fuel, lower ϕ values would be necessary working at higher FR temperatures. Full combustion efficiencies were obtained at both temperatures working at ϕ values above 1.6.

The results obtained in this work showed that the Cu-based material prepared by impregnation can achieve full syngas combustion to CO_2 and H_2O, maintaining high reactivity, and low attrition rate without agglomeration problems after 40 h of continuous operation in the CLC plant.

4. **CONCLUSIONS**

A Cu-based oxygen carrier prepared by impregnation on γ-Al_2O_3 has been tested in a 500 W_{th} CLC pilot plant to analyze their behaviour with regard to syngas combustion.

The effect of the main operating conditions, such as the syngas composition, the oxygen carrier to fuel ratio and the fuel reactor temperature has been studied.

The effect of the syngas composition was analyzed for two different CO/H_2 ratios, 1 and 3. For comparison purposes, experiments with pure H_2 and CO as fuel gas were also done. The highest efficiencies were obtained for H_2 and the lowest for the CO due to the low reactivity of the oxygen carrier with this gas. High and similar combustion efficiencies were obtained for the different syngas compositions used, even when the CO content of the fuel gas was very different. These results can be explained considering the water gas shift (WGS) reaction as an intermediate step in the global combustion reaction of syngas.

The fuel reactor temperature and the oxygen carrier to fuel ratio (ϕ) had a great influence on the combustion efficiency of the process. Complete combustion efficiency were found at ϕ values above 1.5 for syngas (CO/H_2=3) even at temperatures as low as 1073 K. Moreover, it was found that the solids inventory has a high relevance on the combustion efficiency. A solid inventory in the FR higher than 400 kg/MW_{th} is necessary to obtain complete combustion. Nevertheless, the solid circulation rate became also an important parameter working at low oxygen carrier to fuel ratios ($\phi <$ 1.4). For ϕ values higher than 1.4, an increase in the solids inventory in the FR had higher influence on the combustion efficiency than an increase in the solids circulation rate.

After 40 hours of operation in the prototype, the oxygen carrier exhibited an adequate behaviour regarding processes such as attrition, agglomeration and carbon deposition. It can be concluded that the Cu-based oxygen carrier prepared by impregnation could be used with high efficiency in a CLC plant for syngas combustion.

Acknowledgements

This research was conducted with financial support from the Spanish Ministry of Science and Innovation (MICINN, Project CTQ2007-64400). C. R. Forero thanks UNIZAR-BSCH for the predoctoral fellowship.

NOMENCLATURE

f_S = flow of solids in the CLC system (kg h^{-1})

F_i = molar flow of the i compound (mol s^{-1})

m_{ox} = mass of the oxidized form of the oxygen carrier (kg)

m_{red} = mass of the reduced form of the oxygen carrier (kg)

m^*_{FR} = solids inventory in the fuel reactor referred to 1 MW_{th} (kg MW^{-1})

R_{OC} = oxygen transport capacity of the oxygen carrier, as defined in Eq. (4)

T = temperature (K)

w_0 = CuO content in the oxygen carrier (wt.%)

x_i = molar fraction of the gas i

X_r = reduction conversion of the oxygen carrier in the FR

Greek symbols

ΔX_S = variation of the solid conversion, as defined in Eq. (10)

ϕ = oxygen carrier to fuel ratio, as defined in Eq. (7)

λ = air excess ratio, as defined in Eq. (5)

η_c = combustion efficiency, as defined in Eq. (6)

Subscripts

AR = Air reactor

FR = Fuel reactor

REFERENCES

[1] Climate Change 2007: Mitigation of Climate Change. Contribution of Working Group III to the Fourth Assessment Report of the Intergovernmental Panel on Climate Change, Cambridge University Press, Cambridge, U.K., 2008 (available at www.ipcc.ch).

[2] H. R. Kerr, Capture and separation technologies gaps and priority research needs, in: *Carbon Dioxide Capture for Storage in Deep Geologic Formations-Results from the CO_2 Capture Project*, D. Thomas, S. Benson (Eds.), Elsevier Ltd., Amsterdam, The Netherlands, 2005, Vol. 1, Chapter 38.

[3] IPCC Special Report on Carbon Dioxide Capture and Storage. Prepared by Working Group III of the Intergovernmental Panel on Climate Change, Cambridge University Press, Cambridge, U.K., 2005 (available at www.ipcc.ch).

[4] A. Abad, J. Adánez, F. García-Labiano, L.F. de Diego, P. Gayán, J. Celaya, Mapping of the range of operational conditions for Cu-, Fe-, and Ni-based oxygen carriers in chemical-looping combustion, *Chem. Eng. Sci*. 62 (2007**)** 533–49.

[5] A. Lyngfelt, H. Thunman, Construction and 100 h operational experience of a 10-kW chemical-looping combustor, in: *Carbon Dioxide Capture for Storage in Deep Geological Formations- Results from the CO_2 capture Project*. D. Thomas, S. Benson (Eds.), Elsevier Ltd., Amsterdam, The Netherlands, 2005, Vol. 1, Chapter 36.

[6] J. Adánez, P. Gayán, J. Celaya, L.F. de Diego, F. García-Labiano, A. Abad, Chemical-looping combustion in a 10 kW prototype using a CuO/Al_2O_3 oxygen

carrier: effect of operating conditions on methane combustion, *Ind Eng Chem Res*. 45 (2006) 6075-6080.

[7] L.F. de Diego, F. García-Labiano, P. Gayán, J. Celaya, J.M. Palacios, J. Adánez, Operation of a 10 kWth chemical-looping combustor during 200 h with a CuO-Al2O3 oxygen carrier, *Fuel* 86 (2007) 1036-1045.

[8] C. Linderholm, A. Abad, T. Mattisson, A. Lyngfelt, 160 hours of chemical-looping combustion in a 10 kW reactor system with a NiO-based oxygen carrier, *International Journal of Greenhouse Gas Control* 2 (2008) 520-530.

[9] H.J. Ryu, G.T. Jin, C.K. Yi, Demonstration of inherent CO_2 separation and no NOx emission in a 50 kW chemical-looping combustor: Continuous reduction and oxidation experiment, in: *Proceedings of the Seventh International Conference of Greenhouse Gas Control Technologies*, M. Wilson, T. Morris, J. Gale, K. Thambibutu (Eds.). *Elsevier Ltd*., Oxford, UK, 2005, vol. 2, p. 1907.

[10] K. Mayer, T. Pröll, J. Bolhar-Nordenkampf, P. Kolbitsch, H. Hofbauer, Chemical Looping Combustion in a 120 kW test rig- First results, in: *Proceedings 9th International Conference on Fluidized Beds*, Hamburg, Germany, 2008.

[11] Y.Cao, W.P.Pan, Investigation of Chemical Looping Combustion by Solid Fuels. 1. Process Analysis, *Energy Fuels 20* (2006) 1836-1844.

[12] S.A. Scott, J.S. Dennis, A.N. Hayhurst, T. Brown, In situ gasification of a solid fuel and CO_2 separation using chemical looping, *AIChE J. 52(9)* (2006) 3325-3328.

[13] J.B. Yang, N.S. Cai, Z.S. Li, Reduction of Iron Oxide as an Oxygen Carrier by Coal Pyrolysis and Steam Char Gasification Intermediate Products, *Energy Fuels* 21(6) (2007) 3360-3368.

[14] H. Leion, T. Mattisson, A. Lyngfelt, Solid Fuels in Chemical-Looping Combustion, *International Journal of Greenhouse Gas Control* 2 (2008) 180-193.

[15] R. J. Copeland, G. Alptekin, M. Cessario, Y. Gerhanovich, A Novel CO_2 Separation System, in: Proceedings of the First National Conference on Carbon Sequestration, Washignton, DC, 2001, available in the web: *http://www.netl.doe.gov/publications/proceedings/01/carbon_seq/carbon_seq01.html.*

[16] H. Jin, M. Ishida, A new type of coal gas fueled chemical-looping combustion, *Fuel* 83 (2004) 2411-2417.

[17] J. Wolf, M. Anheden, I. Yan, Performance of power generation processes with Chemical-Looping Combustion for CO removals requirements for the oxidation and reduction reactors, *International Pittsburgh Coal Conference*, Newcastle, New South Wales, Australia, Dec 3-7, 2001.

[18] A. Abad, T. Mattisson, A. Lyngfelt, M. Rydén, Chemical-looping combustion in a 300 W continuously operating reactor system using a manganese-based oxygen carrier, *Fuel* 85 (2006**)** 1174-1185.

[19] E. Johansson, T. Mattisson, A. Lyngfelt, H. Thunman, Combustion of syngas and natural gas in a 300 W chemical-looping combustor, *Chem. Eng. Res. and Design* 84 (A9) (2006) 819 – 827.

[20] A. Abad, T. Mattisson, A. Lyngfelt, M. Johansson, The use of iron oxide as oxygen carrier in a chemical-looping reactor, *Fuel* 86 (2007**)** 1021–1035.

[21] C. Dueso, F. García-Labiano, J. Adánez, L. F. de Diego, P. Gayán, A. Abad, Syngas combustion in a chemical-looping combustion system using an impregnated Ni-based oxygen carrier, Fuel (2009), doi:10.1016/j.fuel.2008.11.026.

[22] A. Abad, F. García-Labiano, L. F. de Diego, P. Gayán, J. Adánez, Reduction kinetic of Cu-, Ni-, Fe-based oxygen carriers using syngas ($CO+H_2$) for Chemical-Looping Combustion, *Energy & Fuels* 21 (2007) 1843-1853.

[23] J. Adánez, L. F. de Diego, F. García-Labiano, P. Gayán, and A. Abad, Selection of Oxygen Carriers for Chemical-Looping Combustion, *Energy & Fuels,* 18 (2) (2004) 371 -377.

[24] L. F. de Diego, F. García-Labiano, J. Adánez, P. Gayán, A. Abad, B. M. Corbella, J. M. Palacios, Development of Cu-based Oxygen Carriers for Chemical-Looping Combustion, *Fuel* 83 (2004) 1749-1757.

[25] L. F. de Diego, P. Gayán, F. García-Labiano, J. Celaya, A. Abad, J. Adánez, Impregnated CuO/Al_2O_3 oxygen carries for chemical-looping combustion: avoiding fluidized bed agglomeration, *Energy Fuels* 19 (2005) 1850-1856.

[26] F. García-Labiano, P. Gayán, J. Adánez, L. F. de Diego, C.R. Forero, Solid Waste Management of a Chemical-Looping Combustion Plant using Cu-Based Oxygen Carriers, *Environ. Sci. Technol.* 41 (16) (2007) 5882 -5887.

[27] F. García-Labiano, L. F. de Diego, J. Adánez, A. Abad, P. Gayán, Reduction and Oxidation Kinetics of a Copper-Based Oxygen Carrier Prepared by Impregnation for Chemical-Looping Combustion, *Ind. Eng. Chem. Res.* 43 (2004) 8168-8177.

[28] S.C. Stultz, J.B. Kitto, Steam, its generation and use. 40th ed., *Babcock & Wilcox*. Barbeton, Ohio, 1992.

FIGURE CAPTIONS

Fig. 1 - (a) Schematic diagram of the continuous Chemical-Looping Combustion plant and (b) Typical pressure profile of the installation. Numbers show the location of the pressure transducers.

Fig. 2 - Effect of fuel on the reactivity of the fresh Cu-based oxygen carrier at 1073 K.

Fig. 3 - Gas product distribution obtained at the outlet of FR and AR during a typical test for the Cu-based oxygen carrier. Test 16: CO/H_2=3; T_{FR} = 1073 K; T_{AR} = 1223 K ; ϕ = 2.0.

Fig. 4 - Attrition rate versus time for the Cu-based oxygen carrier.

Fig. 5 - Effect of the gas composition on the combustion efficiency for the Cu-based oxygen carrier. T_{FR} = 1073 K, T_{AR} =1223 K. ϕ=1.4. ○ : Syngas; □ : H_2; △ : CO

Fig. 6- CO and H_2 concentrations obtained at the outlet of the FR during syngas combustion in the continuous CLC plant. T_{FR} = 1073 K, T_{AR} = 1223 K.

Fig. 7 - Effect of the oxygen carrier to fuel ratio (ϕ) on the combustion efficiency (η_c) for different fuel gas. Experimental tests where the solids circulation rate (f_s) was varied. T_{FR} = 1073 K, T_{AR} = 1223 K.

Fig. 8 - Effect of the oxygen carrier to fuel ratio (ϕ) on the combustion efficiency (η_c) for different fuel gas. Experimental tests where the fuel flow (▬) or the solids circulation rate (▪▪▪) were varied T_{FR} = 1073 K, T_{AR} = 1223 K. Values indicate the solids inventory per MW, m^*_{FR} .

Fig. 9 - Effect of the FR temperature on the combustion efficiency for the Cu-based oxygen carrier. CO/H_2 = 3. Results from experimental tests where the fuel flow was varied.

TABLES

Table 1 - Properties of the Cu-based OC as prepared (fresh) and used for 40 h in the CLC prototype.

Table 2 - Composition of the gas used during reduction in the TGA experiments. T=1073 K ; P= 1 bar.

Table 3 - Composition of the gas fuel and main data for the experiments carried out in the continuous CLC plant.

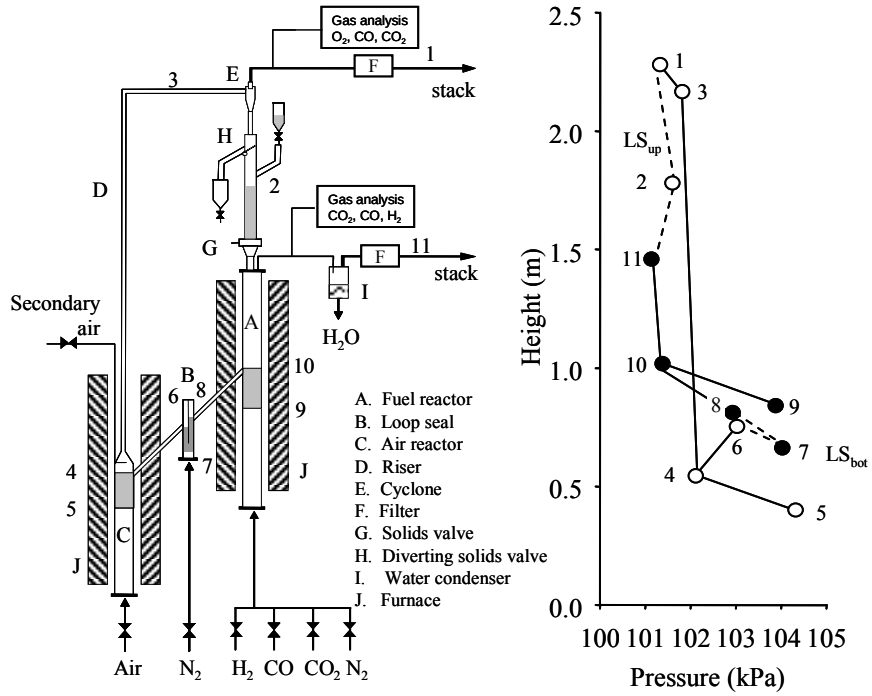

Fig. 1 - (a) Schematic diagram of the continuous Chemical-Looping Combustion plant and (b) Typical pressure profile of the installation. Numbers show the location of the pressure transducers.

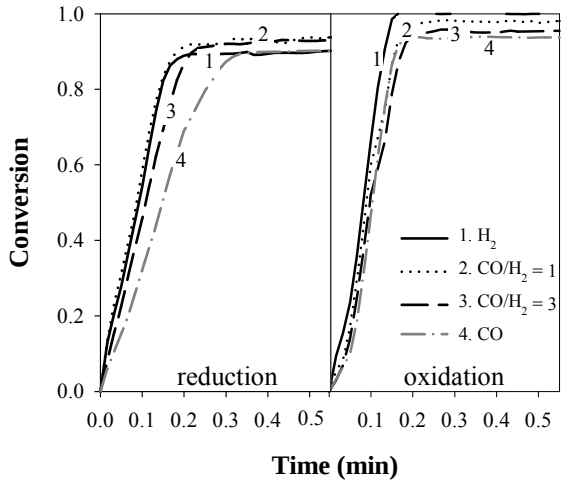

Fig. 2 - Effect of fuel on the reactivity of the fresh Cu-based oxygen carrier at 1073 K.

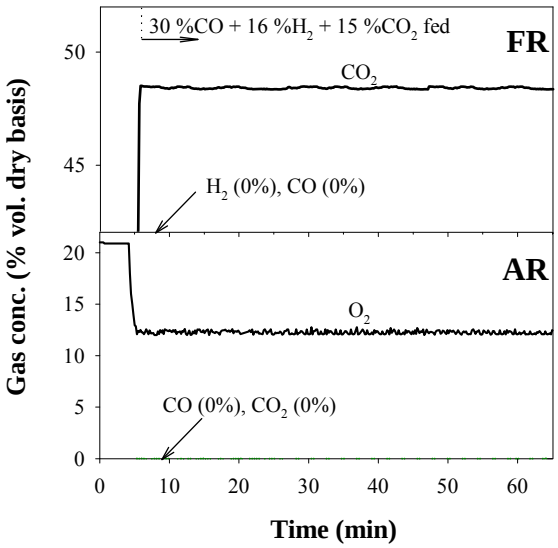

Fig. 3 - Gas product distribution obtained at the outlet of FR and AR during a typical test for the Cu-based oxygen carrier. Test 16: CO/H_2=3; T_{FR} = 1073 K; T_{AR} = 1223 K ; ϕ = 2.0.

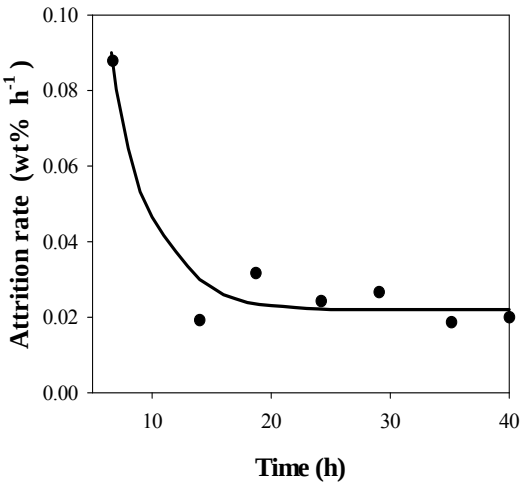

Fig. 4 - Attrition rate versus time of the Cu-based oxygen carrier.

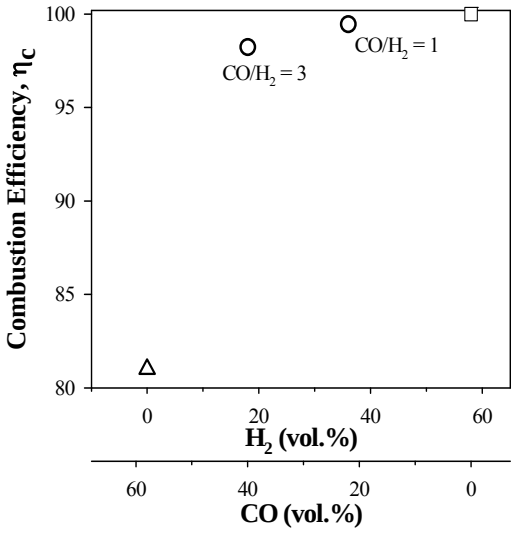

Fig. 5 - Effect of the gas composition on the combustion efficiency for the Cu-based oxygen carrier. T_{FR} = 1073 K, T_{AR} =1223 K. ϕ=1.4. ○ : Syngas; □ : H_2; △ : CO

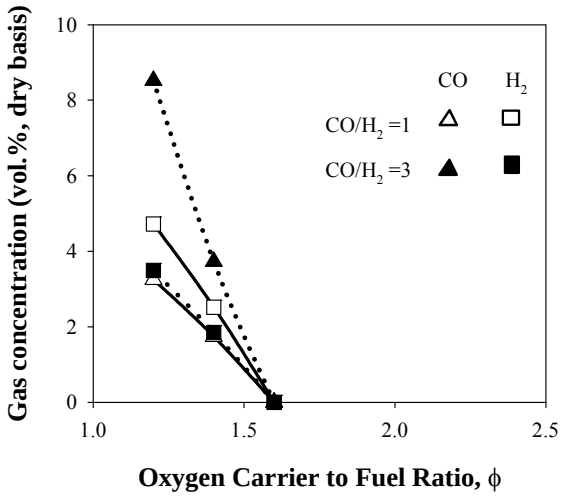

Fig. 6- CO and H_2 concentrations obtained at the outlet of the FR during syngas combustion in the continuous CLC plant. T_{FR} = 1073 K, T_{AR} = 1223 K.

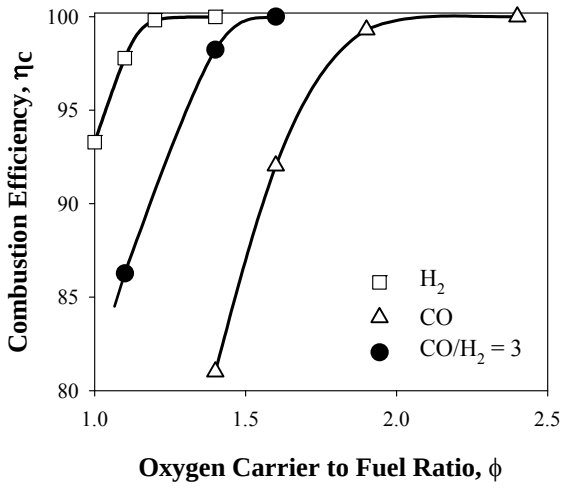

Fig. 7 - Effect of the oxygen carrier to fuel ratio (ϕ) on the combustion efficiency (η_c) for different fuel gas. Experimental tests where the solids circulation rate (f_s) was varied. T_{FR} = 1073 K, T_{AR} = 1223 K.

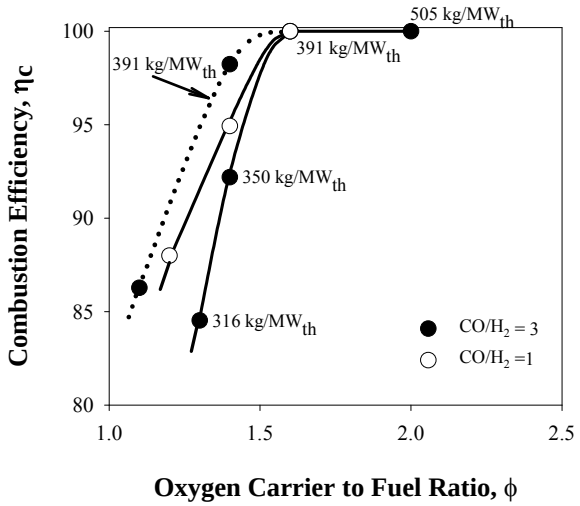

Fig. 8 - Effect of the oxygen carrier to fuel ratio (ϕ) on the combustion efficiency (η_c) for different fuel gas. Experimental tests where the fuel flow (—) or the solids circulation rate (▪▪▪) were varied T_{FR} = 1073 K, T_{AR} = 1223 K. Values indicate the solids inventory per MW, m^*_{FR} .

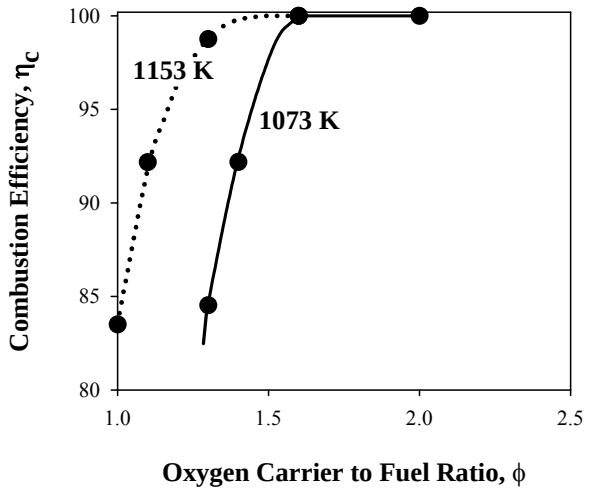

Fig. 9 - Effect of the FR temperature on the combustion efficiency for the Cu-based oxygen carrier. $CO/H_2 = 3$. Results from experimental tests where the fuel flow was varied.

Table 1 - Properties of the Cu-based OC as prepared (fresh) and used for 40 h in the CLC prototype.

	fresh	used
Active material, w_o (wt%)	13.9	13.5
Oxygen transport capacity, R_{OC}: (%)	2.8	2.7
Particle size (μm)	0.3 – 0.5	0.3 – 0.5
Particle density (g/cm^3)	1.6	1.9
Porosity (%)	50	50
Specific surface area BET (m^2/g)	77	5.3
Crushing strength (N)	2.4	1.8
XRD phases	CuO, $CuAl_2O_4$, γAl_2O_3	CuO, $CuAl_2O_4$, $CuAlO_2$, αAl_2O_3

Table 2 - Composition of the gas used (vol.%) during reduction tests in the TGA experiments. T=1073 K; P= 1 bar.

Test	CO	H_2	H_2O	CO_2	CO/H_2 ratio
Pure CO	15			15	
Syngas 1	7.5	7.5	10	11	1
Syngas 3	11.2	3.8	10	33	3
Pure H_2		15			

Table 3 - Composition of the gas fuel used and main data for the experiments carried out in the continuous CLC plant.

Test	T_{FR}	Gas Fed (vol.%)[a]		Equilibrium conditions (vol.%)				CO/H_2	Power	ϕ	fs	m^*_{FR}
	(K)	CO	H_2	CO	H_2	CO_2	H_2O		(W_{th})		(kg/h)	(kg/MW)
Variation of gas composition												
1	1073	40	18	44	14	11	4	3	511	1.4	5.2	391
2	1073	22	36	29	29	8	7	1	491	1.4	5.2	407
3	1073		58		58				453	1.4	5.2	442
4	1073	58		58		15			529	1.4	5.2	378
Variation of solids circulation rate (f_s) with syngas												
5	1073	40	18	44	14	11	4	3	511	1.6	6.0	391
6	1073	40	18	44	14	11	4	3	511	1.1	4.3	391
Variation of solids circulation rate (f_s) with pure gases												
7	1073		58		58				453	1.2	4.2	442
8	1073		58		58				453	1.1	4.0	442
9	1073		58		58				453	1.0	3.8	442
10	1073	58		58		15			529	2.4	8.9	378
11	1073	58		58		15			529	1.9	7.1	378
12	1073	58		58		15			529	1.6	6.0	378
Variation of fuel flow at two CO/H_2 ratios												
13	1073	22	36	29	29	8	7	1	491	1.6	6.0	407
14	1073	25	40	32	32	8	7	1	542	1.4	6.0	369
15	1073	28	42	35	35	8	7	1	593	1.2	6.0	338

16	1073	30	16	34	11	11	4	3	396	2.0	6.0	505
17	1073	45	20	49	16	11	4	3	572	1.4	6.0	350
18	1073	50	22	54	18	11	4	3	633	1.3	6.0	316
Variation of FR Temperature												
19	1153	30	16	34	11	11	4	3	396	1.6	5.2	505
20	1153	40	19	44	15	11	4	3	519	1.3	5.2	386
21	1153	48	22	52	17	11	4	3	607	1.1	5.2	329
22	1153	56	24	61	20	11	4	3	713	1.0	5.2	281

[a] 15 vol% CO_2 and N_2 for balance were also fed.